CHAPTER 3

LUNAR OCCULTATION STUDIES OF 63 RADIO SOURCES

This chapter presents a study of 63 weak radio sources with a median flux density of about 0.5 Jy at 326.5 MHz from their lunar occultations observed with the Ooty Radio Telescope. Accurate positions and brightness distributions along a minimum of two position angles have been derived for these sources from their occultation profiles. Optical identification is attempted from the Palomar Sky Survey Prints for all the sources. Brightness distributions of the sources were derived by using both Scheuer's method and the Optimum Deconvolution Method (ODM), and significant differences in the results obtained from these methods are pointed out.

3.1 OBSERVATIONS AND ANALYSIS OF DATA

3.1.1 Observations: The Ooty Radio Telescope and its special design features for observing lunar occultations have been described by Swarup et al. (1971), and the details of observation and analysis of data have been described by Swarup et al. (1971a), Kapahi et al. (1973), Kapahi(1975a) and Gopal-Krishna (1976).

Lunar occultations of the sources presented in this chapter were observed during 1970-71 with the Ooty telescope operating at 326.5 MHz with a bandwidth of 4 MHz and a receiver time constant of 1 sec. At least two occultations were observed for all the 63 sources (a single immersion or emersion is being referred to here as an occultation). Some of the sources were also observed during 1973-74 and the data from these occultations have also been included. Since

a reliable digital recording system was completed only by late 1971, the data were digitised manually from chart records at intervals of 1 to 3 sec depending on the chart speed. The effects of time constant, bandwidth and sampling interval of the digitised data have been taken into account in determining the effective resolutions of the restored brightness distributions.

3.1.2 Radio Positions : The time of occultation of a source defines its position as lying on the instantaneous topocentric limb of the Moon. From two such occultations we can infer the position of the source as one of the intersections of the corresponding limbs of Moon. The choice between these two positions is made by using the approximate declination which can be inferred to within $\sim$1 arc min by comparing the deflections in successive beams with the known beam pattern of the Ooty telescope in declination (Kapahi 1975a). The details of computation of the position from the occultation times have been given by Sutton (1966).

For computing the radio positions and occultation parameters of the sources described in this chapter, the lunar ephemeris j = 2 has been used, and the positions have been referred to the FK4 equinox. Corrections for limb-irregularities are determined from the charts published by Watts(1963).

3.1.3 Optical Positions: The search for optical objects in the fields of the 63 radio sources was made on the prints of the Palomar Sky Survey. The identification was decided on the basis of positional agreement, peculiarity of the optical object and the radio structure derived from occultation

measurements. In order to measure the coordinates of the optical objects, contact plates were made from the Sky Survey Prints for the regions of the radio sources. From these plates, the X - Y coordinates of the optical object of interest and about 10 to 15 reference stars within about 1^{o} of the object were measured to within a few microns using the Zeiss Coordinate Measuring Machine. The reference stars were selected from the SAO Star Catalogue and the positions of the objects close to the radio source were computed from their X - Y coordinates by the method of dependences (van de Kamp 1967, Ch 7). The optical positions so derived have an rms error of about 0.5 arc sec in each coordinate as inferred from a measurement of the coordinates of 25 quasars for which published positions were available to an accuracy of 0.3 to 0.4 arc sec (Kapahi et al. 1973). If the image of the object was too faint to register on the contact plate, its coordinates were estimated from a direct measurement of its distances from several neighbouring brighter objects. For such objects, the derived coordinates have an rms error of about 2 arc sec.

3.1.4 Radio Structure . The one-dimensional strip scans of the brightness distributions of the sources were derived from the occultation profiles by Scheuer's method (Section 1.3.3) as well as the ODM (Chapter 2). However, the results based on ODM are presented only when they are significantly different from those obtained by Scheuer's method.

3.2 POSITION, STRUCTURE AND IDENTIFICATION

3.2.1 Structure of the Sources : The structural details of the 63 sources derived from their occultation profiles are given in Table 3.1, arranged as follows.

Column 1 : Source number in the Ooty code (standard RA-Dec code prefixed by OTL). Other catalogue numbers, if any, are given in parentheses.

Column 2 : Total flux density at 326.5 MHz. The estimated rms errors are 15 - 25 per cent.

Column 3 : The number of occultations used in the analysis.

Column 4 : Position Angle of Scan (PA)

Column 5 : Method on which the structural information is based - ODM or Scheuer's Method (SCH).

Column 6 : Highest effective resolution (β_e) used

Columns 7 and 8 : Derived structure along the PA given in Col. 4. Sizes prefixed by are likely to have been resolved, but have somewhat larger errors ($\sim$ 30 per cent).

Columns 9 to 11 : Derived Parameters for double sources. Errors in the listed position angles of separation from A to B (Col 9) and in the separation between the components (Col 10) depend on those given for positions in Table 3.2. The flux-ratios (Column 11) are generally accurate to $\pm$ 0.2.

Column 12 : Remarks. The symbol '(N)' indicates that additional notes or comments are given in the text. The other symbols used are :
Cx = Complex ; D = Double ;
PD = Possibly Double.

Table 3.1 : Structural data from occultations of 63 radio sources

Source name (OTL)	S_{327}	No. of occ	PA	METHOD	Observed data: θ_e	Comp. sizes: A	Comp. sizes: B	Derived str.: PA (A to B)	Comp. sep.	S_A/S_B	Remarks
1	2	3	4	5	6	7	8	9	10	11	12
0004+040	0.5	2	109°	SCH	4"	4"					PD(SCH)
				ODM	2	≲ 2	≲ 2	177°	6"	1.5	
			173	SCH	8	8					
				ODM	4	4	≲ 3				
0006+046 (0B+013)	1.0	4	65	SCH	15	20					(N)
			198	SCH	10	15					
			208	SCH	15	16					
			219	SCH	15	15					
0022+072	0.5	2	74	SCH	15	23					PD in PA 230°
			230	SCH	15	18					
0046+103 (MC2)	1.2	2	48	SCH	20	25		12	30	1.1	(N)
			246	SCH	20	22					
0050+102 (4C 10.03,MC2)	1.0	2	56	SCH	10	13					
			85	SCH	20	25					
0057+105 (4C 10.04,MC2)	1.0	2	106	SCH	1.4	1.7					
			179	SCH	1.3	1.3					
0117+138	0.3	2	22	SCH	5	< 5					
			270	SCH	20	22					
0123+140 (4C 13.08)	1.3	6	102	SCH	3	3.5	9	130	12	2.5	(N)
			209	SCH	1.5	1.0	2				
0319+236 (OE 232)	0.7	3	55	SCH	15	30			> 30		D (N)
			78	SCH	15	23					
0322+238	0.3	2	70	SCH	6	5					
			266	SCH	15	< 12					
0325+238	0.3	2	99	SCH	20	≲ 20					
				ODM	12	10					
			249	SCH	20	30					
0358+251 (B2)	0.4	2	125	SCH	10	< 10					
			235	SCH	20	20					
0433+262 (B2)	1.5	2	124	SCH	12	≲ 10	14				
				ODM	10	10	10	136	18	0.8	
			246	SCH	4	< 4	< 4				
				ODM	3	3	3.7				

1	2	3	4	5	6	7	8	9	10	11	12
0434+269	0.6	4	35	SJH	5	< 4					
			119	SJH	2.2	≲ 2					
			205	SJH	2.2	≲ 2					
0439+269	0.2	2	124	SJH	10	≲ 8					
			219	SJH	10	≲ 8					
				ODM	8	8					
0445+273 (B2)	0.4	2	254	SJH	15	≲ 15					
			344	SJH	4	< 4					
0450+270	0.5	2	132	SJH	20	15					
			236	SJH	15	12					
0453+272 (B2)	0.3	3	83	SJH	15	< 15					
0500+270 (B2)	1.2	3	116	SJH	2.1	3.5					
			250	SJH	2.2	2.3					(N)
			323	SJH	4	< 4					
0502+275	0.3	2	66	SJH	5	≲ 5					
				ODM	2.5	4					
			304	SJH	15	12					
0544+273 (B2)	0.3	2	140	SJH	10	≲ 10					
			245	SJH	10	≲ 10					
0558+264 (B2)	0.7	2	128	SJH	30	30					
			219	SJH	10	14					
0559+271 (B2)	0.3	2	63	SJH	8	≲ 8					
				ODM	2.5	6					PD(ODM)
			293	SJH	3.2	< 3					
0559+268 (B2)	0.4	4	31	SJH	10	< 8					
			39	SJH	5	< 4					
			151	SJH	2.2	< 2					
			205	SJH	5	< 4					
0719+248 (B2)	0.4	2	70	SJH	30	35					(N)
			311	SJH	10	≲ 10					
0814+201 (H 0814+20)	0.5	2	94	SJH	15	12	–				(N)
				ODM	4	< 4	6	80	12	1.5	
			327	SJH	15	≲ 15	–				
				ODM	4	< 4	< 4				
0902+162	0.3	2	106	SJH	4	< 4					
				ODM	3	≲ 3					
			332	SJH	8	≲ 8					
				ODM	6	10					

1	2	3	4	5	6	7	8	9	10	11	12
0946+118	0.9	2	131	SJH	8	$\lesssim$ 8					PD(ODM)
				ODM	4	6					
			287	SJH	8	$\lesssim$ 8					
				ODM	4	6					
1040+062	2.0	2	10	SJH	8	$\lesssim$ 12	$\lesssim$ 12	99	15	1.4	(N)
			80	SJH	4	5	3.5				
1107+036	1.8	2	148	SJH	3	7	10	86	64	2.5	(N)
(HM 1107+03.6)			300	SJH	3	12	15				
1225-083	1.7	2	178	SJH	4	$<$ 4	$<$ 4	103	14	1.7	
(HM 1225-08?)				ODM	1.5	$<$ 1.5	1.7				
			243	SJH	8	$\lesssim$ 8	12				
				ODM	4	6	12				
1242-101	0.8	6	168	SJH	2.1	$<$ 2					
			228	SJH	2.1	$\lesssim$ 2					
			256	SJH	8	$\lesssim$ 8					
			296	SJH	5	$<$ 5					
1257-113	1.3	3	112	SJH	6	23	6	113	50	0.7	Bridge with
			244	SJH	8	23	12				25% flux
			336	SJH	4	$\lesssim$ 4	10				
1300-121	0.7	2	128	SJH	1.4	$<$ 1					
			293	SJH	1.3	$<$ 1					
1310-133	1.6	4	128	SJH	8	$\lesssim$ 7	$\lesssim$ 7	43	35	1.4	Bridge with
				ODM	3	2.5	$\lesssim$ 2				15% flux
			140	SJH	4	$\lesssim$ 4	$\lesssim$ 4				
			278	SJH	2.2	3.2	2.1				
			291	SJH	2.2	2.2	$<$ 2				
1357-180	1.3	3	103	SJH	2.2	$\lesssim$ 2					
				ODM	2	$\lesssim$ 2					
			147	SJH	3.3	$\lesssim$ 3					
				ODM	2	2					
			252	SJH	8	$<$ 8					
				ODM	4	$<$ 4					
1411-192	1.5	7	122	SJH	4	4.5	4	7	14	1.5	
(MC1)			136	SJH	6	$\lesssim$ 6	$<$ 6				
				ODM	3	4	$\lesssim$ 3				
			273	SJH	2	$\lesssim$ 2					
1430-204	0.3	2	86	SJH	15	$<$ 15					
				ODM	6	$<$ 6					
			346	SJH	8	$\lesssim$ 8					
				ODM	6	$\lesssim$ 5					
1526-248	0.3	2	160	SJH	5	5.5					
			245	SJH	10	$<$ 8					

1	2	3	4	5	6	7	8	9	10	11	12
1556-262	0.6	2	181	SJH	8	10					PD(SJH)
				ODM	4	5	5.5	115	25	2.0	
			223	SJH	6	6					
				ODM	4	5	6				
1652-270 (PKS)	1.6	2	41	SJH	4	$\lesssim$ 4	$\lesssim$ 4	93	19	1.0	Bridge with 15% flux
			305	SJH	8	8	12	(165)	(21)		
1703-275	0.3	2	55	SJH	12	12					
			285	SJH	12	$\lesssim$ 12					
1713-279	0.6	2	109	SJH	15	$\lesssim$ 12	$\lesssim$ 12	156	35	1.5	
				ODM	6	$\lesssim$ 6	$\lesssim$ 6				
			245	SJH	4	$\lesssim$ 4	$\lesssim$ 4				
1721-280	0.7	2	154	SJH	8	10	—				Single in
				ODM	2	2	3	154	5	0.5	SJH
			228	SJH	3	$\lesssim$ 3	—				
1722-280	0.6	2	137	SJH	8	8					
			239	SJH	15	20					
1754-276	0.4	2	78	SJH	5	$\lesssim$ 5					
				ODM	2	3					
			291	SJH	3	$\lesssim$ 3					
				ODM	2	$\lesssim$ 2					
1832-269	0.3	2	110	SJH	10	$\lesssim$ 8					
				ODM	4	$\lesssim$ 4					
			207	SJH	10	$\lesssim$ 8					
1832-265	0.6	2	36	SJH	8	6					
			281	SJH	15	16					
1837-262	1.2	2	30	SJH	8	8					
			64	SJH	2.5	2					
1900-259	0.7	2	57	SJH	15	14					
			266	SJH	4	$\lesssim$ 4					
1905-253	0.4	2	39	SJH	30	$\lesssim$ 25					
				ODM	20	18					
			270	SJH	10	$\lesssim$ 8					
				ODM	6	$\lesssim$ 5					
1907-256	0.4	2	34	SJH	8	$\lesssim$ 6					
			319	SJH	8	$\lesssim$ 8					
1928-237	0.5	2	78	SJH	15	25					
			225	SJH	15	$\lesssim$ 15					PD(ODM)
				ODM	6	6					

1	2	3	4	5	6	7	8	9	10	11	12
1951-232 (OV-286)	0.5	2	50	SJH	4	< 4					
			268	SJH	8	< 8					
1952-234	0.3	2	120	SJH	8	< 8					
			192	SJH	15	≤ 12					
				ODM	8	9					
2023-200	0.7	2	74	SJH	4	4					
			216	SJH	6	7					
2050-186	0.3	2	21	SJH	8	< 8					
			272	SJH	8	< 8					
2058-181	0.4	2	96	SJH	4	< 3					
			210	SJH	8	< 8					
2119-169 (PKS)	2.5	2	65	SJH	8	≲ 7					(N)
			256	SJH	4	≲ 4					
2219-092	1.0	2	68	SJH	2	≲ 2					
			221	SJH	4	< 4					
2232-062	0.8	2	3	SJH	15	12					(N)
			292	SJH	15	15					
2235-073	0.6	2	43	SJH	8	< 8					
			248	SJH	2	≲ 2					
2255-046	0.7	2	32	SJH	15	12					
			239	SJH	15	17					

3.2.2 Position and Identification : The radio positions and the details of associated optical objects are summarised in Table 3.2, arranged as follows:

Column 1 : Source number (OTL)

Columns 2 to 5 : Right Ascension (Col. 2), Declination (Col. 4) and their standard errors (Cols. 3 and 5). For complex or possibly double sources, the tabulated positions refer to the centroid of emission. These are marked by '(C)' before the position. The symbol 'a' in Cols. 3 and 5 indicates that the position errors are specified better along the two perpendicular position angles given in the footnotes to the Table.

Column 6 : Galactic latitude (b^{II}), to the nearest degree.

Columns 7 and 8 : Optical positions of the nearest object. Generally, these positions have errors of $\sim \pm$ 0.5 arc sec, but those underlined have uncertainties of about 2 arc sec in each coordinate. The positions enclosed in parentheses were estimated directly from the overlays to an accuracy of about 5 arc sec. Optical positions have not been listed for crowded fields and blank fields with no interesting object within 30 arc sec of radio.

Column 9 : Photographic magnitudes of the optical objects estimated visually from the Sky Survey Prints. The red prints were generally used except for the magnitudes enclosed in parentheses which refer to the blue Prints. Positive or likely identifications are indicated by an asterisk just before the Column.

Column 10 : Notes on optical objects. The symbol '(N)' refers to additional comments in the text.

Table 3.2 Coordinates of 63 Sources and Notes on Optical Identifications

Source OTL	Position (1950) Radio					Optical		m_{pg}	Notes on optical objects
	α	$\Delta\alpha$	δ	$\Delta\delta$	b^{II}	α	δ		
1	2	3	4	5	6	7	8	9	10
0004+040	$0^h\ 04^m\ 54^s.57$	$\pm 0^s.1$	$+04^\circ\ 05'\ 09''.4$	$\pm 1''.5$	-57°	$54^s.97$	$05'\ 09''.9$	$*20^m$	gal in cl.
0006+043	00 06 44.87	0.1	+04 41 18	2	-56	45.88	41 14.4	*17.5	gal in cl (N)
0022+072	00 22 07.8	0.2	+07 14 43	4	-55	07.89	14 38.7	*20	red gal
0046+103	00 46 45.75	a	+10 18 06	a	-52	45.84	18 05.5	19	star
0050+102	00 50 17.50	0.15	+10 12 30	2	-52				
0057+105	00 57 28.71	0.04	+10 32 56.2	0.6	-52				
0117+138	01 17 51.24	0.2	+13 50 23	2	-48				
0123+140 A	01 23 33.21	0.07	+14 04 44.0	1.0	-48	33.46	04 38.9	*20	blue gal
B	33.87	0.1	04 36.0	1.0					
Jen	33.48	0.07	04 39.9	1					
0319+236 Jen	3 19 41.1	0.2	+23 40 16	5	-27	40.69	40 29.4	19	only in blue
0322+238	03 22 33.43	0.15	+23 50 34.	5	-27	33.62	50 35.3	*20.5	only in red
0325+238	03 25 50.49	0.15	+23 51 07	5	-26	49.69	50 56.7	20.5	red only
0358+251	03 58 33.25	0.2	+25 07 54	3	-20	33.83	07 59.0	17	gal in cl.
0433+262 A	04 33 20.91	0.08	+26 15 33.3	1.5	-14				
B	21.75	0.1	25	2					
Jen	21.50	0.1	30	2					
0434+269	04 34 07.73	0.06	+26 56 11.8	0.8	-13				
0439+269	04 39 56.1	0.2	+26 57 46	3	-12				
0445+273	04 45 11.5	0.2	+27 23 30	3	-11				
0450+270	04 50 41.3	0.2	+27 01 50	3	-10				
0453+272	04 53 28.0	0.2	+27 12 11	3	-10	27.41	12 14.1	18.5	Star
0500+270(J)	5 00 51.02	0.06	+27 04 48.1	1	- 9	(50.3)	(04 48)	20.5	red only

1	2	3	4	5	6	7	8	9	10
0502+275	05 02 11.8	0.2	+27 33 44	3	-08	09.88	33 39.9	19.5	red only(N)
0544+273	05 44 25.8	0.2	+27 20 56	3	00	(25.4)	(21 13)	18	star
0558+264	05 58 35.2	0.25	+26 25 50	3	+02				crowded field
0559+271	05 59 38.85	0.1	+27 11 43	2	+02	(38.8)	(11 22)	20.5	red only
0559+268	05 59 50.25	0.07	+26 51 03.8	1	+02				crowded
0719+248	07 19 39.8	0.2	+24 51 33	3	+18	39.64	51 36.3	18.5	red db?(N)
0814+201 A	08 14 11.39	0.15	+20 08 02	3	+28	12.25	08 04.4	*20	stellar,
B	12.26	0.15	08 04	3					only in
Gen	11.62	0.1	08 00	2					red
0902+162	09 02 40.4	0.2	+16 16 46	3	+37	39.70	17 07.2	18.5	gal?
0946+118	09 46 59.3	0.2	+11 48 31	4	+45				
1040+062 A	10 40 14.31	0.15	+06 14 22	2	+53	18.47	13 51.0	17	E-gal
B	15.33	0.15	14 20	2					
Gen	14.82	0.15	14 22	3					
1107+036 A	11 07 48.3	0.2	+03 37 52	3	+56	50.51	37 56.3	*17	blue gal
B	52.59	0.1	37 57	3		49.25	37 53.6	19	NSO (N)
Gen	49.0	0.25	37 49	5					
1225-083 A	12 25 45.21	0.08	-08 21 37.2	1	+54	45.42	21 38.1	*18.5	N-gal ?
B	46.14	0.08	21 40	3					
Gen	45.57	0.1	21 38.2	1					
1242-101	12 42 43.42	0.1	-10 09 59.3	1.5	+52	43.59	09 56.3	12	NSO
1257-113 A	12 57 16.8	0.3	-11 21 22	6	+51				
B	16.9	0.3	21 42	6					
Gen	15.6	0.2	21 26	3					
1300-121	13 00 24.4	a	-12 07 07	a	+50	23.83	06 56.7	18.5	star
1310-133 A	13 10 11.84	0.1	-13 18 56	3	+49				
B	13.46	0.1	18 30	2	+49				
Gen	12.57	0.05	18 44.1	1					
1357-130	13 57 30.00	0.06	-18 04 58.0	1	+42				
1411-192 A	14 11 36.34	0.05	-19 14 02	1.5	+39	36.04	13 46.7	17	BSO ?
B	36.46	0.05	13 48	1.5					
Gen	36.39	0.05	13 59.6	1					
1430-204	14 30 51.18	0.15	-20 25 44.5	2	+36	51.90	25 32.2	20.5	(N)
1526-248	15 26 31.4	0.2	-24 48 29	3	+26				

1	2	3	4	5	6	7	8	9	10
1556-262	A 15 56 07.78	0.1	-26 17 48.8	1.5	+20	07.52	17 46.0	20.5	db? only
	B 09.43	0.15	59	2.5					in red
	Gen 08.08	0.1	50.2	1.5					
1652-270	Gen 16 52 07.0	0.2	-27 01 32	3	+10				crowded
1703-275	17 03 02.7	0.2	-27 31 15	4	+08				crowded
1713-279	A 17 13 00.49	0.1	-27 58 01	2	+06				crowded
	B 01.55	0,15	58 33						
	Gen 01.06	0.15	58 18	2					
1721-280	17 21 08.45	0.1	-28 03 24.2	1.5	+04				crowded
1722-280	17 22 11.8	0.2	-28 02 47	3	+04				crowded
1754-276	17 54 34.85	0.1	-27 41 45	1.5	- 2				crowded
1832-269	18 32 08.1	0.2	-26 56 57	2	-09				crowded
1832-265	18 32 24.0	0.2	-26 35 05	3	-08				crowded
1837-262	18 37 24.52	0.1	-26 17 02	2	-14				crowded
1900-259	19 00 00.09	0.1	-25 57 19	3	-14				crowded
1905-253	19 05 50.75	0.1	-25 19 55	3	-15				crowded
1907-256	19 07 37.06	0.1	-25 37 51	3	-15	(37.5)	(37 40)	18.5	star
1928-237	19 28 07.9	0.2	-23 44 48	3	-19	07.47	44 50.0	18.5	star (20 obj. in ±1')
1951-232	19 51 21.57	0.15	-23 16 22.4	1	-24	(22.2)	(16 17)	15	star
1952-234	19 52 36.15	0.2	-23 29 34	3	-24	(36.0)	(29 55)	19.5	star
2023-200	20 23 09.7	0.3	-20 02 55	3	-29				
2050-186	20 50 00.5	0.2	-18 37 14	3	-35				
2058-181	20 58 50.76	0.1	-18 07 48.5	1.5	-37				
2119-169	21 19 21.05	a	-16 54 36	a	-41	(20.2)	(54 42)	17.5	star
2219-092	22 19 09.67	0.1	-09 17 07	2	-50				
2232-062 (C)	22 32 31.32	0.15	-06 14 11	2	-51	30.32	14 05.9	*(19)	BSO (N)
2235-073	22 35 34.85	0.15	-07 18 38	3	-53	36.86	17 44.8	14	gal in cl.
2255-046	22 55 37.8	a	-04 41 57	a	-55	37.61	41 52.2	*(19)	BSO

cl. = cluster ; gal = galaxy ; db = dumb-bell galaxy
obj = objects ; NSO = Neutral Stellar Object

a Position errors, 0046+103: ± 1" in PA 48° and ± 5" in PA 138°
1300-121: ± 1" in PA 120° and ± 5" in PA 30°
2119-169 ± 1" in PA 75° and ± 7" in PA 165°
2255-046: ± 1" in PA 59° and ± 5' in PA 149°.

* Positive or likely identification; (N)=Additional notes in text.

3.2.3 Additional Comments on Individual sources .

0006+046 : The source consists of a compact component containing roughly half of the total flux and an extension of about 0.5 arc min roughly towards the $17^m.5$ D-galaxy which is $\sim$ 15 arc sec away from the radio centroid in PA 105°.

0046+103 : At least a quarter of the flux comes from the bridge. The component positions could not be determined uniquely since their intensities are comparable. The alternate pairing of the components would, however, imply a large separation of $\sim$ 1.6 arc min which is inconsistent with the Molonglo observations (Sutton et al. 1974).

0123+140 : The occultation position, based on 6 scans, agrees with the 4C and OHIO positions (Dixon 1970) but is $\sim$ 2 arc min to the west of the position given by Munro(1972). The radio centroid determined from the occultation observations coincides with the 20^m blue object.

0319+236 : This is a weak double source, but its orientation could not be determined since the position angles of all the 3 scans are within 30°. Hence only a lower limit to its angular size is given.

0500+270 : The source consists of a compact component of size $<$ 1 arc sec accounting for about half of the total flux, and an extension of a few arc sec, probably towards northwest. Brightness profiles of this source along PA 116° derived by ODM and Scheuer's method are shown in Fig. 3.2.

0719+248 : The large angular size in PA 70° is due to an extended feature of size $\sim$ 1 arc min surrounding the main component $\lesssim$ 10 arc sec and containing more than half of the total flux (Figure 3.5). The identified object is a close pair of $19^m.5$ red galaxies joined by a faint nebulosity.

0814+201 : The ODM output indicates that the source may be double, in PA 94° with a component separation of $\sim$ 12 arc sec. The source has a spectral index of -0.4 ± 0.1 between 327 and 2700 MHz, as inferred from the flux measurements at 327 MHz (present work), 408 MHz (Swarup and Sutton, private communication), 750 and 1400 MHz (Hoglund 1967) and 2700 MHz (T. K. Menon, private communication). The 20^m red object lies near the eastern edge of the radio source.

1040+062 : Interpretation of the emersion data (PA 10°) was made somewhat uncertain due to the presence of an interference spike near the occultation time. However, the effect of this spurious event was eliminated by requiring consistency with the position measured by Swarup and Sutton at Molonglo (private communication).

1107+036 : A schematic diagram of the source structure derived from the present observations is given in Figure 3.1. Both the radio components are extended. The stronger, western component shows two distinct radio peaks for each of which a pair of possible positions is plotted in the Figure. No emission is detected at 327 MHz from the region between the two components.

2119-169 : Since both the occultation records were partly lost due to interference, higher resolution was not possible.

2232-062 : The source consists of a compact component of size $\lesssim$ 4 arc sec which accounts for about half of the total flux and a westerly extension of size about 15 arc sec pointing towards the BSO.

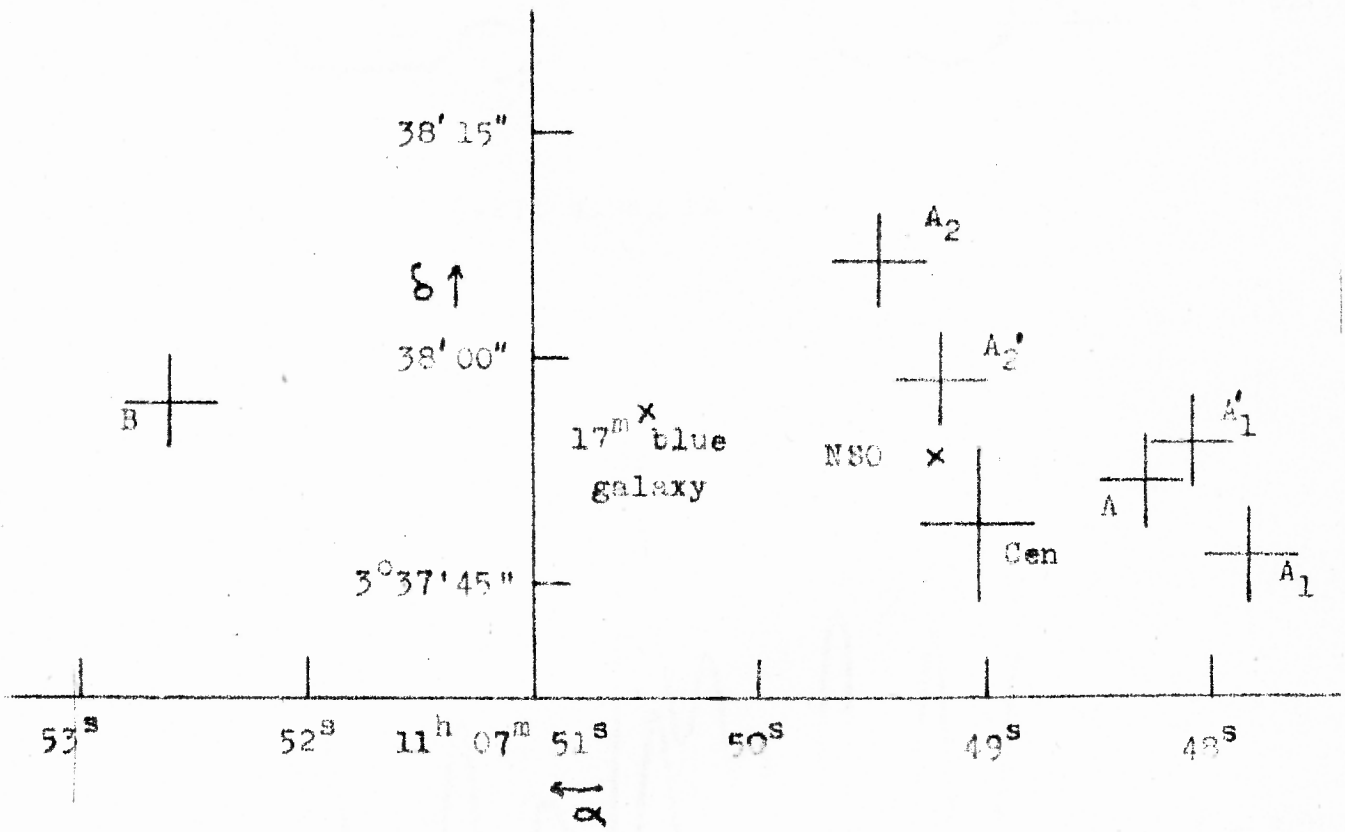

Figure 3.1 : Schematic diagram of the position of the radio components of the source 1107+036 along with the blue galaxy and NSO near the centroid of the source. The positions of optical objects have been taken from Murdoch et al. (1974)

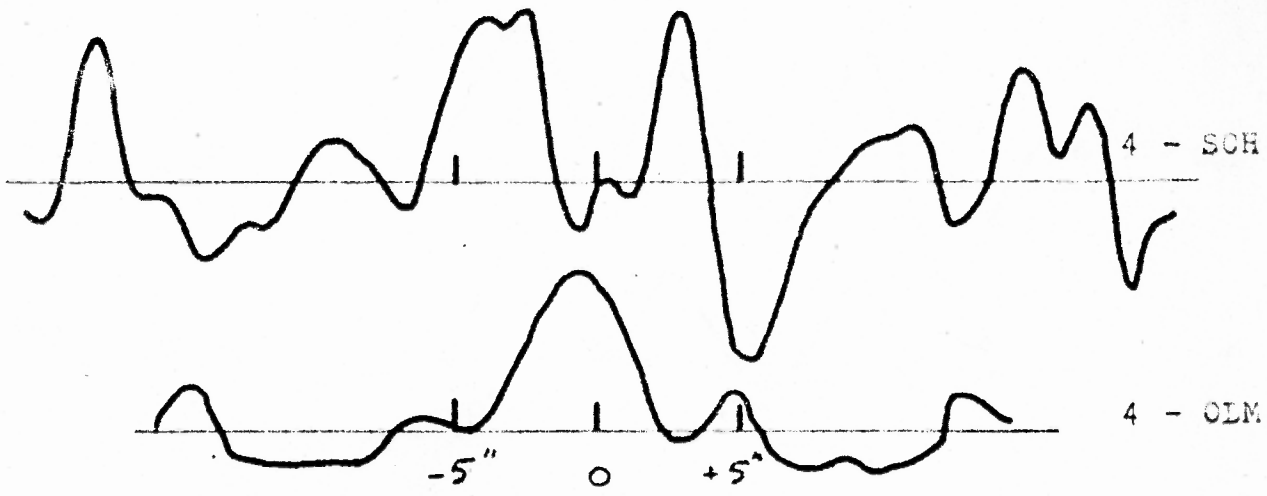

Fig. 3.3 : OTL 0559+271 along PA 63°

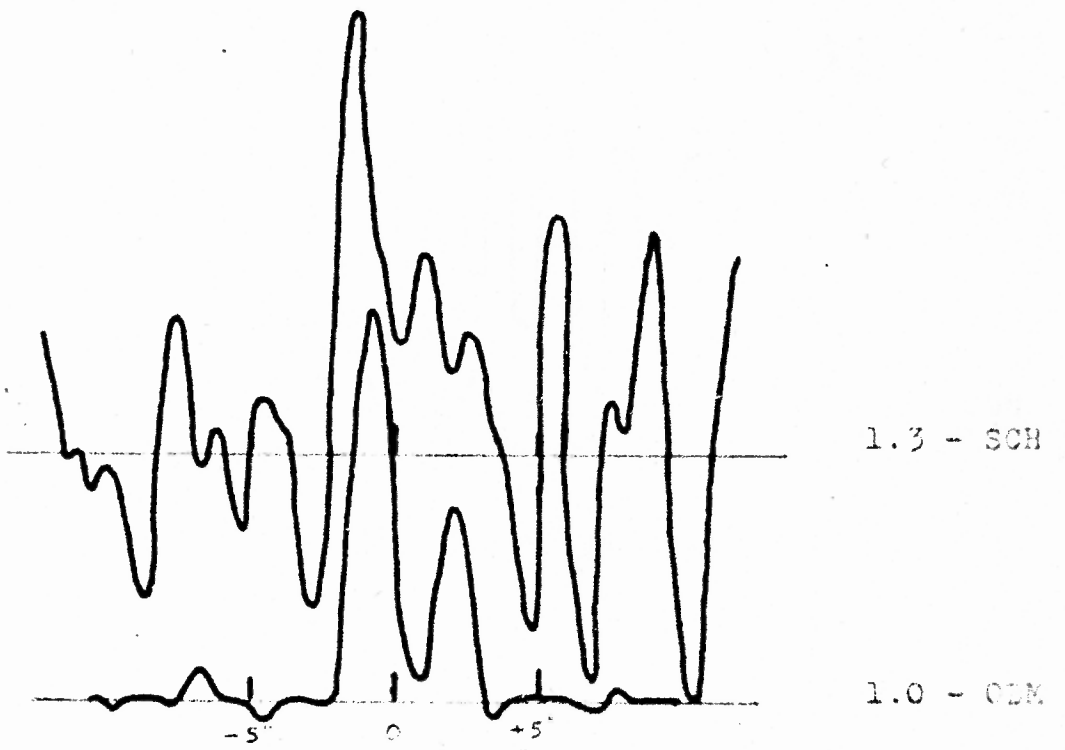

Fig. 3.2 : OTL 0500+276 along PA 116°.
In this and the following Figures, brightness profiles obtained by OLM are compared with those derived from Scheuer's Method (SCH). The numbers on the right of each profile denote the resolution used, in arc sec. The abscissae are labelled in arc sec.

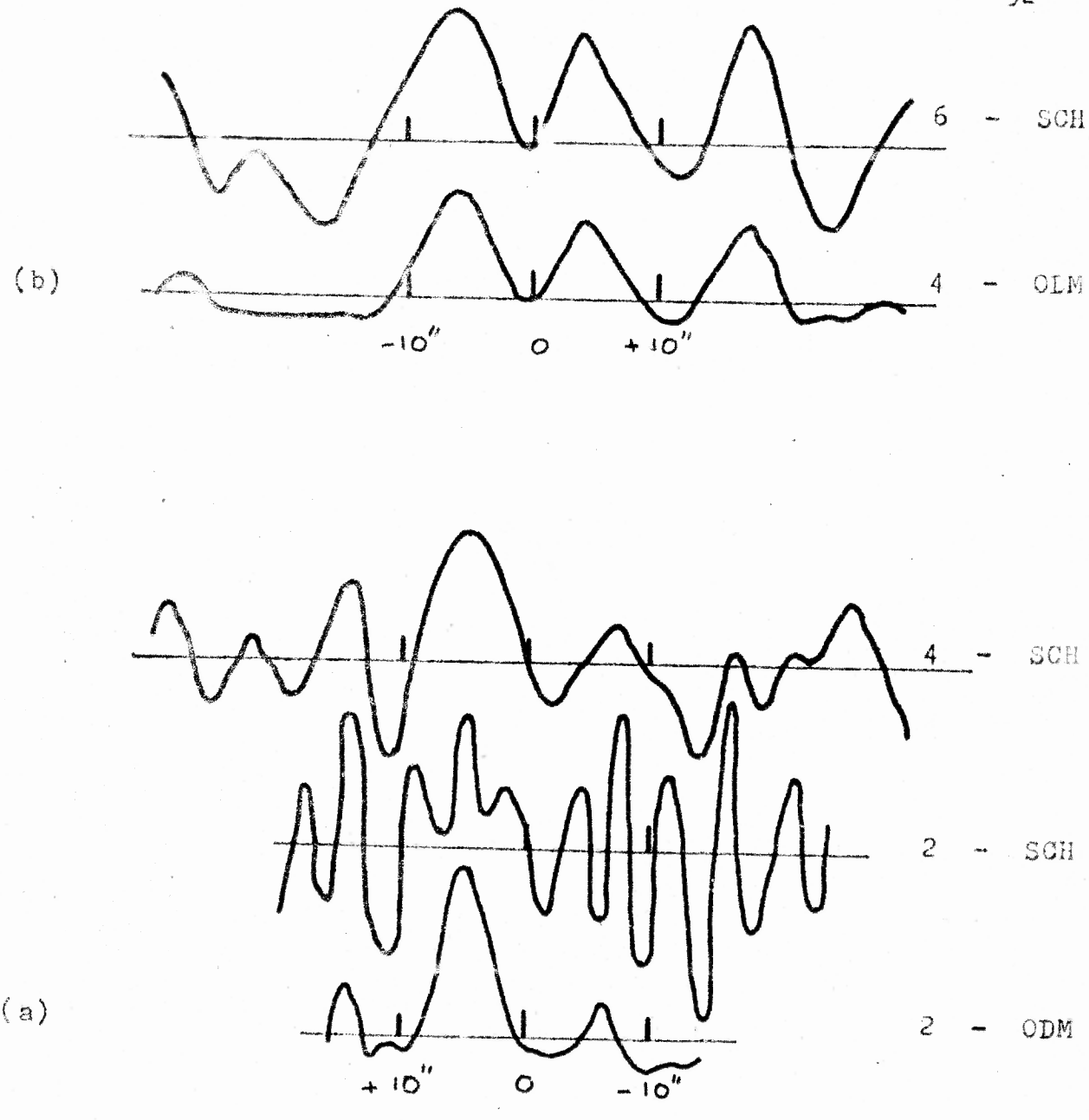

Fig. 3.4 : OTL 0502+275 along PA 66° (a) and 304° (b)

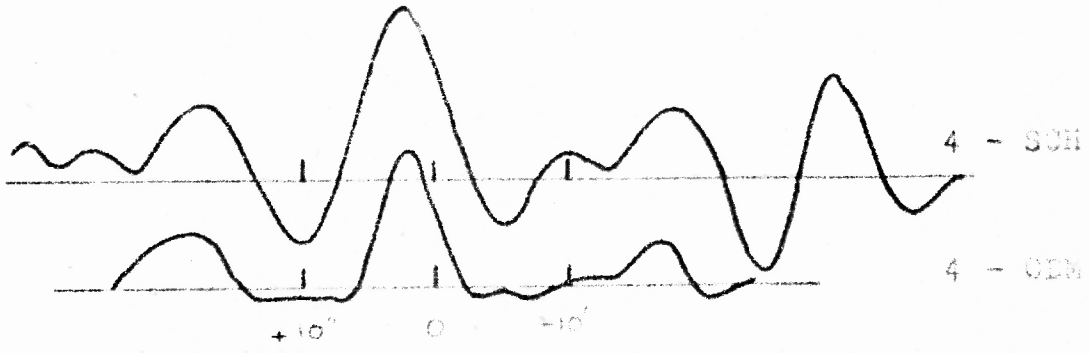

Fig. 3.6 : OTL 0902+062 along PA 106°

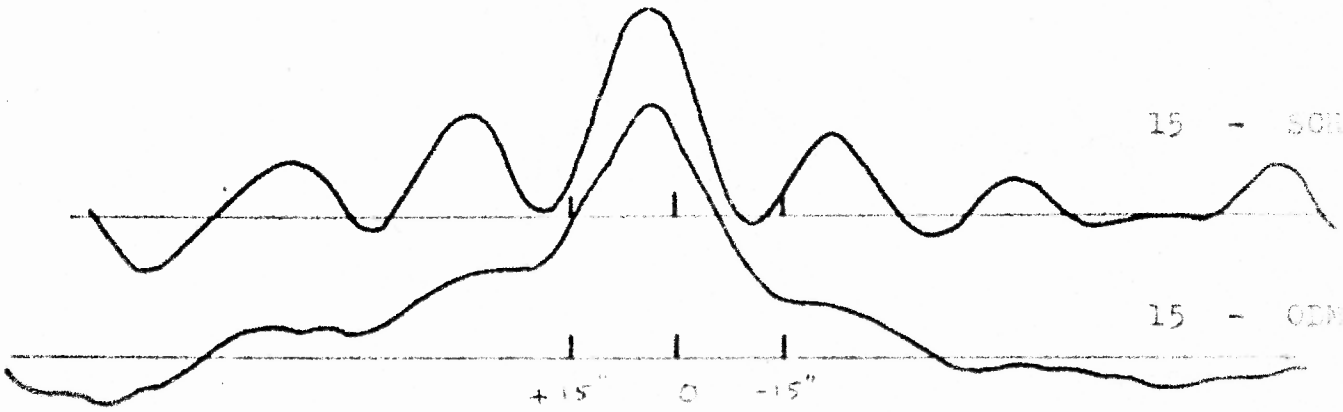

Fig. 3.5 : OTL 0719+248 along PA 70°

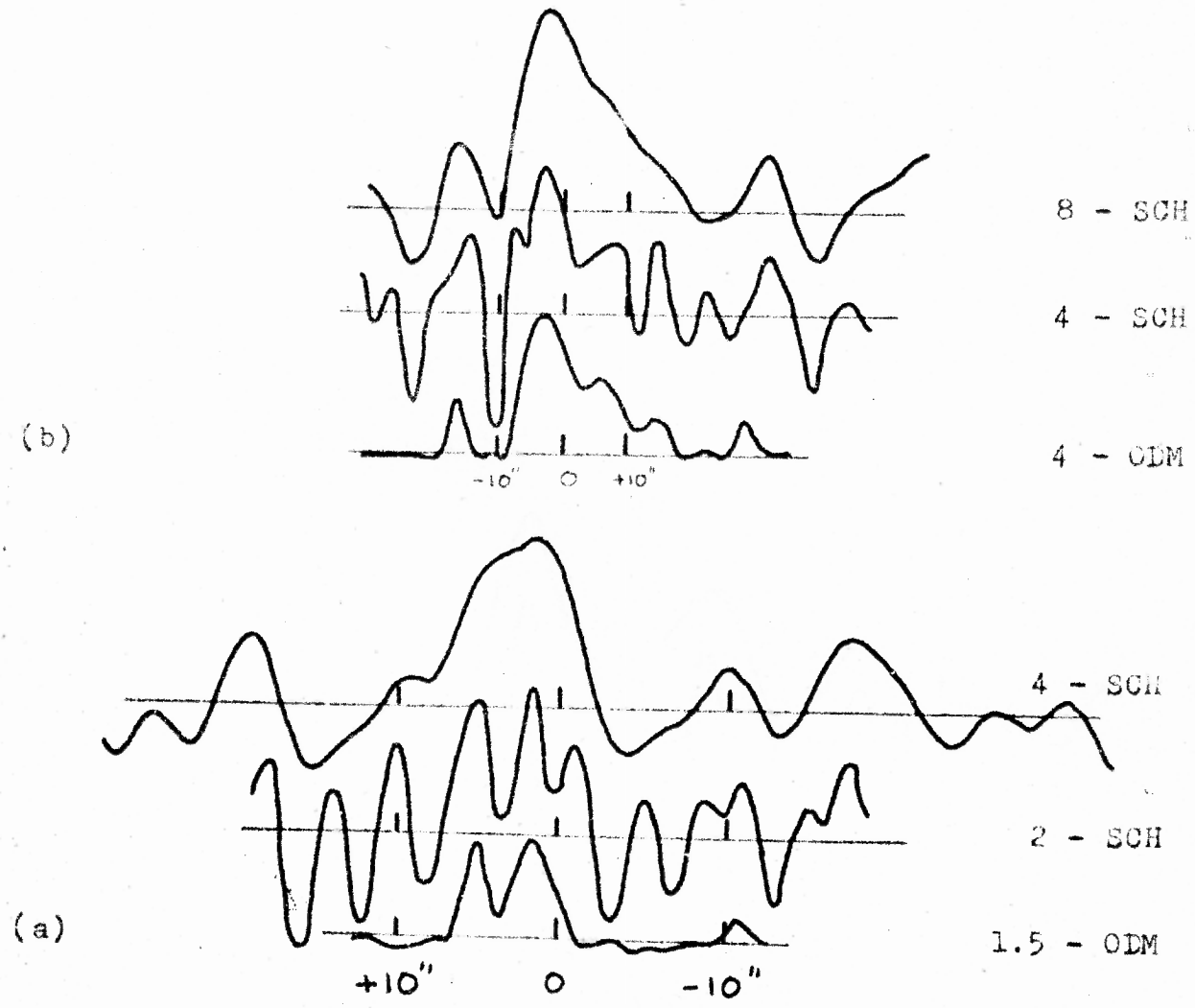

Fig. 3.7 : OTL 1225-083 along PA 178° (a) and 243° (b)

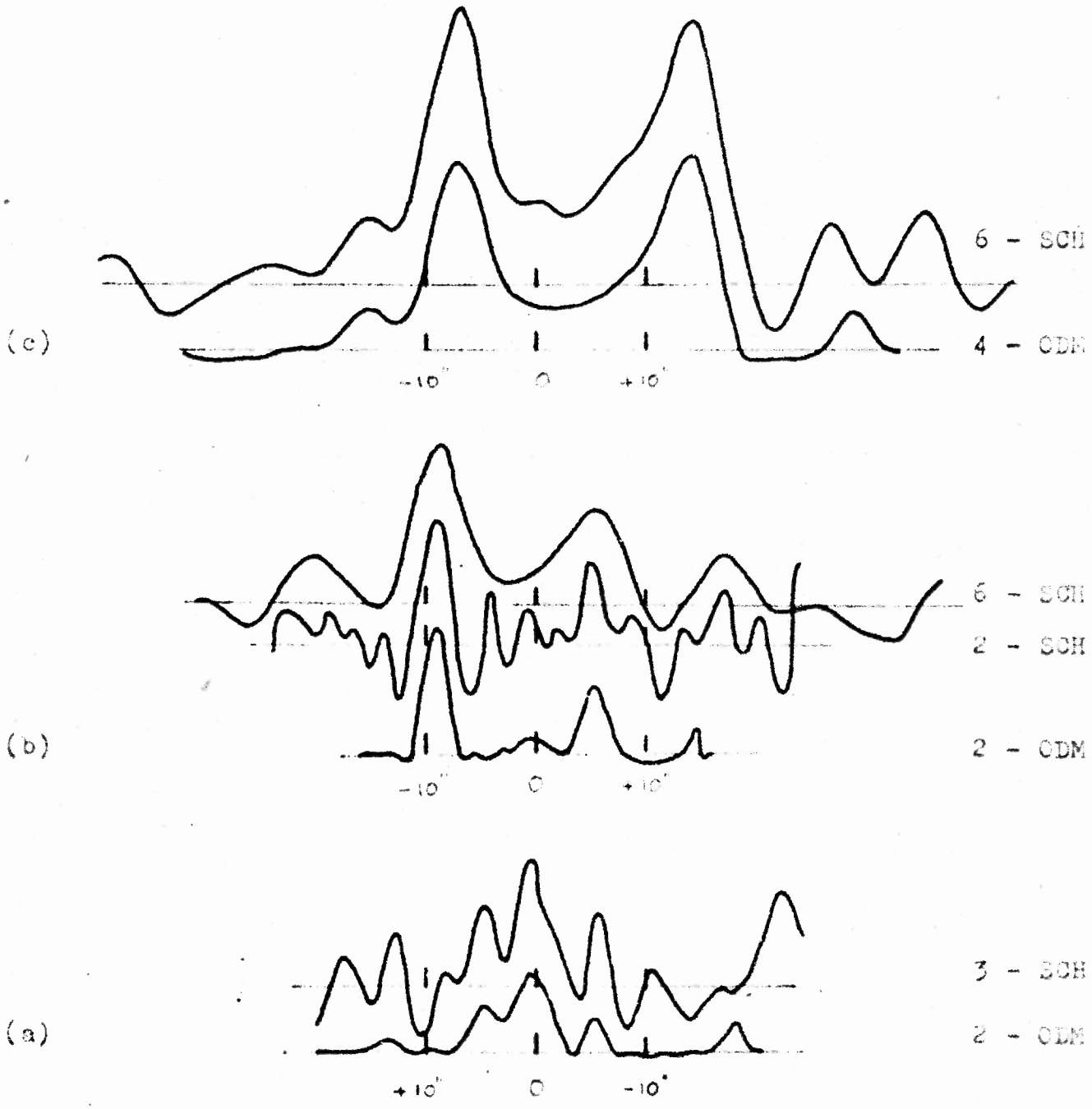

Fig. 3.8 : OTL 1310-133 along position angles:
(a) 128° ; (b) 291° ; and (c) 276°

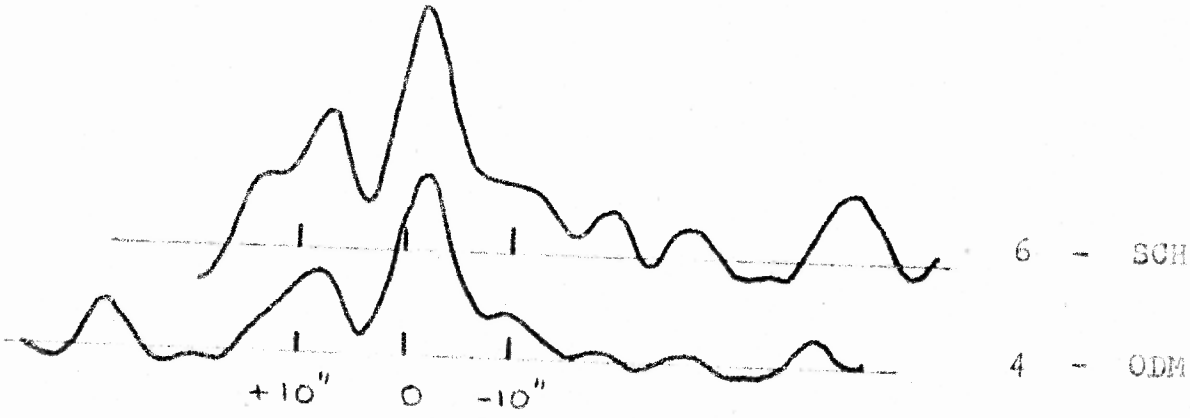

Fig. 3.10 : OTL 1556-262 along PA 181°

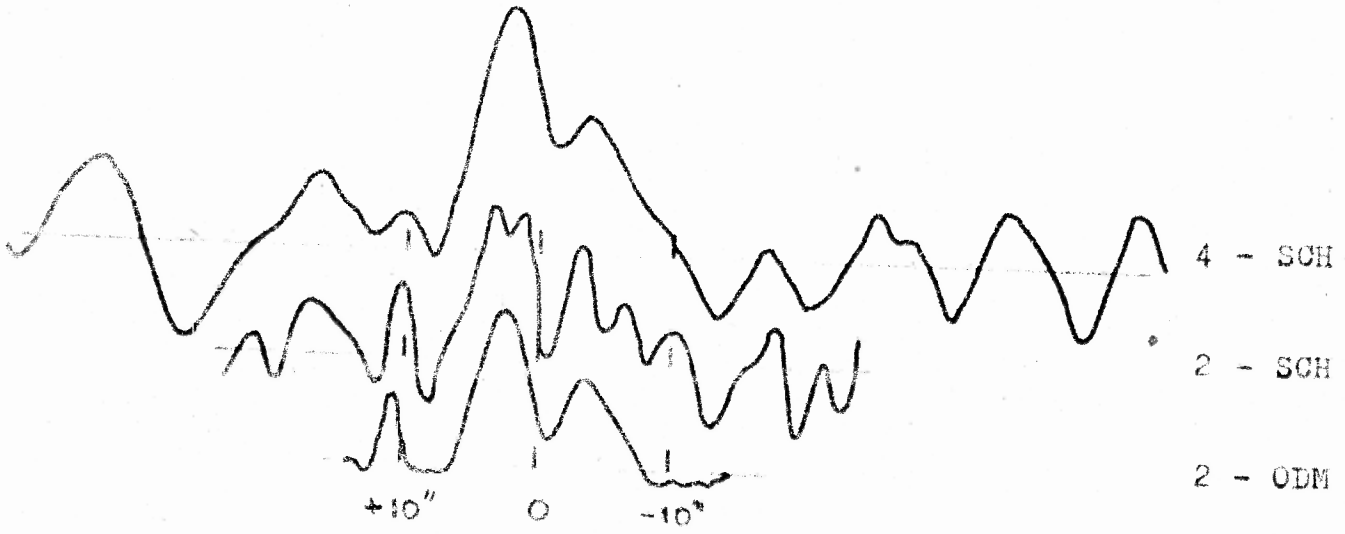

Fig. 3.9 : OTL 1411-192 along PA 122°

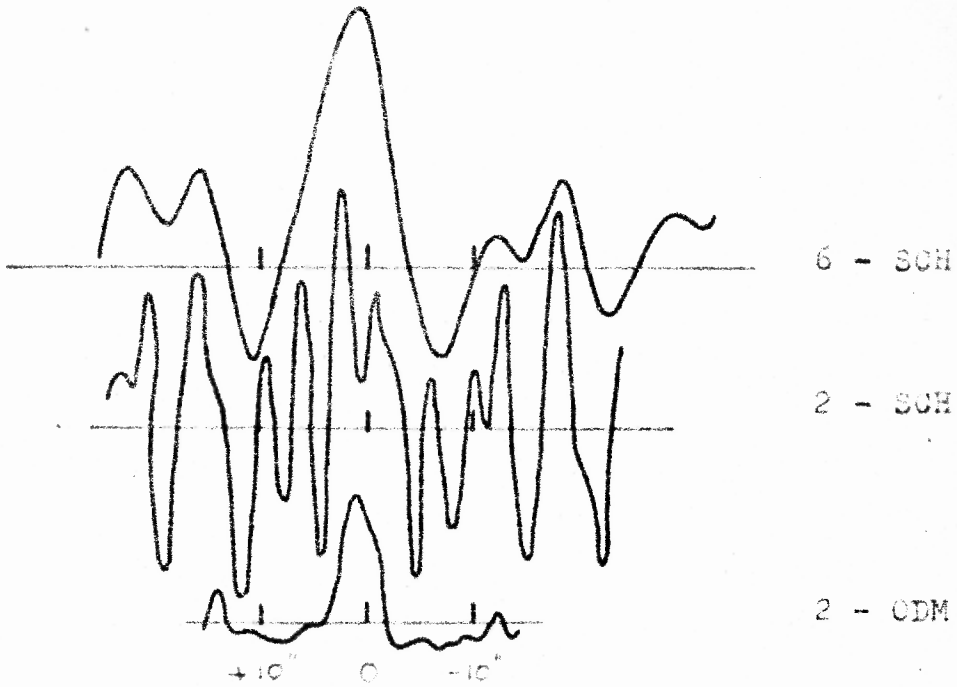

Fig. 3.12 : OTL 1754-276 along PA 78°

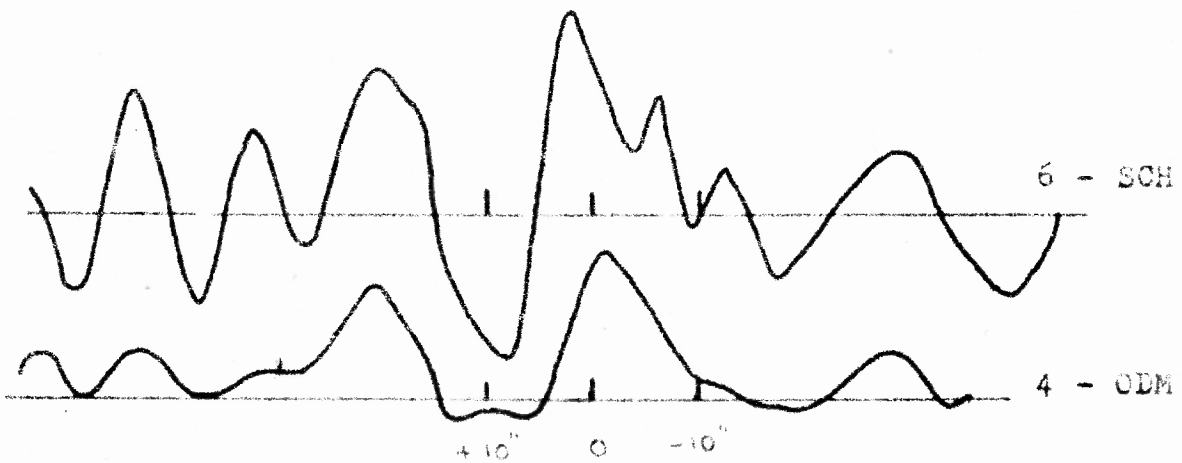

Fig. 3.11 : OTL 1713-279 along PA 109°

3.3 DISCUSSION

3.3.1 Selection of Sources : One of the chief motivations behind selecting the sources presented in this chapter was to judge the applicability of ODM and assess its merit with respect to Scheuer's method for lunar occultations. It was therefore decided to confine ourselves to weak sources observed during 1970-71 with the Ooty Radio telescope. (Fortunately, this was a fairly straightforward selection since the data on stronger sources with good records had anyway been already 'taken away' for the lists published so far!) The 63 sources presented in this chapter have a median flux density of ~0.5 Jy at 326.5 MHz. Out of these, 49 sources have $S_{327} \leq 1$ Jy with a median value of ~ 0.4 Jy. The quality of the observational records used for the present study was generally poor with respect to that of about 500 sources in the Ooty occultation survey which are either published or in preparation for publication. By using ODM on this sample, we are reasonably confident of its general applicability to the reduction of lunar occultation data.

3.3.2 Summary of the Results on Structure and Identification : Out of the 63 sources, 47 (75 per cent) are well-resolved in at least one scan. Of these, 15 are double and 4 more are possibly double. Bridge between the components is clearly seen in 3 of the double sources. Extended emission has been seen in 4 sources in addition to the emission from a compact component. However, they could not be classified into standard morphological types like core-halo or head-tail galaxies.

Optical identifications have been suggested for 12 sources. Of these, 7 are faint objects with $m_{pg} \gtrsim 20^m$. The other 5 are blue objects, one of which is a BSO. Identification could not be attempted for 11 sources lying close to the galactic plane since their fields were either crowded or obscured.

3.3.3 Comparison of ODM and Scheuer's Method : The statistics regarding the structure of the 63 sources based on the information presented in Table 3.1 are summarised in Table 3.3. Restorations performed by using ODM and Scheuer's method are illustrated in Figures 3.2 to 3.12 for 14 occultations of 11 sources presented in this chapter. The convention followed for these illustrations is the same as that adapted in Chapter 2.

Table 3.3 : The Statistics of the Structure of 63 Sources obtained by using ODM and Scheuer's method

Type	All (63 Sources)		$S_{327} \leq 1$ Jy (49 Sources)	
	ODM	SCH	ODM	SCH
Double	15	10	7	3
Possibly Double	4	4	4	3
Marginally resolved	9	12	7	10
Total number of unresolved or marginally resolved sources	16 (29%)	23 (35%)	14 (30%)	20 (41%)

A quantitative assessment of the improvement of ODM over Scheuer's method for these sources is difficult for two reasons. First, we have not been able to define a uniform criterion for determining the finest resolution possible with ODM as can be done in Scheuer's method by specifying an output signal-to-noise ratio of, say 5. Secondly, in a given application, a higher resolution can give more information only if the sources or components are unresolved by conventional methods. Thus the superiority of ODM depends on the structure of sources in the sample and hence is somewhat subjective to this extent.

In order to assess the merit of ODM, we will ignore the 10 sources which were already recognised as double by using Scheuer's method and compare the two methods for the remaining 53 sources. By using ODM on these 53 sources, 5 sources were classified as double and 6 of the completely unresolved sources were well-resolved in at least one scan. Thus there is a significant additional information on at least 11 of these sources (about 20 per cent) by using ODM. In this consideration, we have ignored the improvement obtained by way of resolving the components of double sources or improving the limits to the sizes of unresolved sources.

3.3.4 An Extended Source with Flat Spectrum . The source 0814+201 has a flat spectrum, with $\alpha = -0.4 \pm 0.1$ between 327 and 2700 MHz as inferred from flux-measurements at five frequencies mentioned in the Notes to Table 3.1. Also, a brightness temperature $> 3 \times 10^4$ K is obtained for the parameters given in Table 3.1 corresponding to 326.5 MHz.

These two features of the source characterise a nonthermal origin for the emission. It is therefore interesting that such a nonthermal flat-spectrum source appears clearly resolved at 327 MHz with an overall size of 10 to 15 arc sec. It is possible that the observed flat spectrum of the source results from unresolved components opaque at metre wavelengths, as is often the case. It would be desirable to confirm the origin of the flat spectrum by mapping the source at centimetre wavelengths.

3.3.5 NSO ejected from a Blue Galaxy ? : The source 1107+036 was identified by Hoskins et al. (1972) with the 17^m D-galaxy having a diffuse blue envelope of diameter ~ 20 arc sec showing a bright blue spot in the northern part. But Murdoch et al. (1974) measured its radio position with an accuracy of 2 arc sec and found that it agrees with that of the 19^m neutral stellar object (NSO), located at about 20 arc sec west of the blue galaxy. On the basis of this positional agreement and in view of the existence of a few radio-emitting NSOs which were found to be either high-redshift quasars or BL-Lacertae objects, Murdoch et al. (1974) identified the source 1107+036 with the NSO. However, the basis for this identification is considerably weakened by the structural information derived from the present occultation observations which show the source to be a well-resolved double with both the NSO and the blue galaxy lying close to the axis and near the centre of the two main components of the radio source. Hence an identification of the source with the unusual blue galaxy is consistent with the generally observed morphology of identified double radio sources.

From the present observations, the western radio component is itself resolved into two peaks, as shown in Figure 3.1. It may be noted that one of the radio peaks is separated from the NSO by ~ 5 arc sec which is only 1.5 times the combined rms errors in their positions. Hence it is interesting to verify if the NSO is indeed a radio source and therefore a high-redshift QSO, presumably ejected from the neighbouring blue galaxy. Possibility of such an ejection has been argued by Terrel (1975) based on the recent discovery of BSOs resembling local QSOs at a distance of perhaps 25 kpc from the centre of the galaxy Centaurus A (Blanco et al.1975).

In the absence of a positive radio detection, the NSO is still interesting from its location very close to the line joining the blue galaxy to the western radio component. According to the current ideas on double radio sources (de Young 1976), the transfer of energy from the parent optical galaxy to the outer radio components may also take place in the form of massive objects such as spinars ejected from the galaxy. Hence it would be worthwhile to look for any peculiarities associated with this NSO like (a)radio emission and spectrum; (b) highly redshifted or featureless optical spectrum; or (c)luminous connection between the NSO and the blue galaxy.

3.4 COMMENTS AND CONCLUSIONS

Angular structures have been derived above with resolutions of a few arc sec at 326.5 MHz from the lunar occultation observations of a sample of 63 weak radio sources, selected with a bias towards rejecting good data. The super-resolution

resulting from the use of ODM has led to a revision in the structure of 20 per cent of these sources.

The resolution achievable in lunar occultations depends mainly on the observational signal-to-noise ratio which, in turn, is decided by the sensitivity of the instrument. The sensitivity of the Ooty telescope is expected to be increased by about a factor of 4 in the near future. In addition, the data are now being recorded routinely on magnetic tapes and the computer programmes for analysing them are being updated to incorporate the experience gained over the last few years. It is also planned to use ODM routinely for future reductions of the Ooty occultation data in addition to Scheuer's method. From these, it should be possible to derive angular size information on a large number of weak radio sources with high resolutions of a few arc sec or better at metre wavelengths. In addition to providing valuable statistics useful in cosmological studies of the kind described in the next chapter, this should also provide new data on the structure of subcomponents of radio sources which is important for understanding the physics of their origin and evolution.